Free Radical Biology and Medicine 225 (2024) 236–246

Contents lists available at ScienceDirect

Free Radical Biology and Medicine

journal homepage: www.elsevier.com/locate/freeradbiomed

Cisplatin induces kidney damage through the down-regulation of Prx I by autophagic degradation

Jiyoung Park [a,b,1], Juhyun Sim [a,c,1], Ho Jin Yi [d], Sue Goo Rhee [e], Hyun Ae Woo [a,d,*]

[a] College of Pharmacy, Graduate School of Pharmaceutical Sciences, Ewha Womans University, Seoul, 120-750, South Korea
[b] Fluorescence Core Imaging Center, Department of Life Science, Ewha Womans University, Seoul, South Korea
[c] National Forensic Service, 26460, 10 Ipchun-ro, Wonju, Gangwon-do, South Korea
[d] College of Pharmacy, Graduate School of Applied Science and Technology for Skin Health and Aesthetics, Ewha Womans University, Seoul, 120-750, South Korea
[e] Biochemistry and Biophysics Center, NHLBI, National Institutes of Health, Bethesda, MD, 20892, USA

ARTICLE INFO

Keywords:
Peroxiredoxin I
Cisplatin
ER stress
Nephrotoxicity
Autophagy

ABSTRACT

In this study, we investigated the potential role of PrxI in cis-diamminedichloroplatinum (cisplatin)-induced renal damage in mice. The anticancer drug cisplatin is a chemotherapeutic agent that is widely used to treat solid tumors. Cisplatin-induced nephrotoxicity is a serious dose-limiting side effect, primarily caused by oxidative stress. The oxidative stress further damages DNA, membranes, and mitochondria, and increases endoplasmic reticulum (ER) stress. Cisplatin produces reactive oxygen species (ROS) through Cytochrome P450 2E1 (CYP2E1) and localizes to the surface of the ER, where CYP2E1 is located.

Among the six Prx isoforms, Prx I was selectively degraded in cisplatin-treated kidneys during severe renal function damage. Prx I degradation is blocked in mouse proximal tubular cells treated with 3-methyladenine, an autophagy inhibitor, and in MEF lacking ATG7. Moreover, increased ROS levels on the ER surface due to CYP2E1 overexpression further accelerated Prx I degradation. These results suggest that Prx I degradation is largely mediated through autophagy, which is promoted by cisplatin-induced ER stress. Ablation of Prx I exacerbated cisplatin-induced nephrotoxicity and significantly increased the abundance of oxidative stress, ER stress, and inflammatory markers in the kidney, indicating that Prx I plays a protective role against cisplatin-induced nephrotoxicity.

1. Introduction

Cis-diamminedichloroplatinum (Cisplatin) is a chemotherapeutic drug widely used to treat many solid tumors, including those of the head, neck, lung, testis, ovary, and breast [1,2]. However, among its toxicities including ototoxicity, gastrotoxicity, myelosuppression, and allergic reactions [3], nephrotoxicity is the main dose-limiting side effect. Approximately 20 % of patients receiving high-dose of cisplatin develop severe renal dysfunction. Although DNA-damaging agents such as cisplatin are usually less toxic to non-proliferating cells, they selectively damage proximal tubular cells due to their accumulation in renal cells [4]. Organic cation transporter is critical for cisplatin uptake in the proximal tubules. Despite the belief that DNA damage is the major mechanism underlying cisplatin toxicity [1,5], only approximately 1 % of cisplatin molecules interact with DNA. Therefore, cisplatin cytotoxicity has been suggested to be associated with inflammation, oxidative stress injury, apoptosis through intrinsic caspase activation, and fibrosis.

Recently, endoplasmic reticulum (ER) stress has been reported to be involved in cisplatin cytotoxicity [6–9]. Endoplasmic reticulum (ER) stress is induced by cisplatin and results in increased apoptosis through the induction of pro-apoptotic CCAAT-binding homologous protein [7,8]. Moreover, ER stress induces autophagy [9,10], which is induced by cisplatin *in vivo* [11] and *in vitro* [12–14]. As reactive oxygen species (ROS) on the ER surface can induce ER stress in cisplatin-treated cells [7], we focused on the effects of ROS on cisplatin-induced cytotoxicity and autophagy.

Reactive oxygen species (ROS) has been implicated as an essential cause of cisplatin-induced cytotoxicity [15–17]. It directly act on and

* Corresponding author. College of Pharmacy, Graduate School of Pharmaceutical Sciences, Ewha Womans University, Seoul, 120-750, South Korea.
E-mail addresses: jypark89@ewhain.net (J. Park), jhsim86@korea.kr (J. Sim), yihoz@naver.com (H.J. Yi), rheesg249@yahoo.com (S.G. Rhee), hawoo@ewha.ac.kr (H.A. Woo).
[1] These authors contributed equally to this work.

https://doi.org/10.1016/j.freeradbiomed.2024.09.049
Received 12 August 2024; Received in revised form 15 September 2024; Accepted 29 September 2024
Available online 2 October 2024
0891-5849/© 2024 The Authors. Published by Elsevier Inc. This is an open access article under the CC BY-NC-ND license (http://creativecommons.org/licenses/by-nc-nd/4.0/).

destroy cellular components, including lipids, proteins, and DNA. In the presence of cisplatin, ROS are produced through many pathways, such as NADPH oxidase [18] and mitochondrial pathways [19], inducing renal injury [17,20]. Several antioxidant chemicals that remove ROS have been reported to reduce cisplatin-induced cytotoxicity *in vivo* [21,22]. Although some of these have been studied *in vitro* [16,23], the benefits of endogenous antioxidant enzymes in reducing cisplatin-induced cytotoxicity have not yet been extensively studied *in vivo*.

Among the six isoforms of mammalian Prxs, Prx I is the only enzyme localized to the ER surface [24]. Since Prx I removes ROS produced on the ER surface, Prx I is considered to be involved in cisplatin-induced ER stress. Therefore, we investigated the role of Prx I in cisplatin-induced cytotoxicity and found that Prx I is involved in autophagy induced by ER stress during cisplatin-induced cytotoxicity and is degraded. Prx I deficiency augments cisplatin-induced nephrotoxicity by increasing ER and oxidative stress.

2. Materials and methods

2.1. Cisplatin-induced kidney failure model

Prx I −/− mice were used as previously described [24]. Prx I +/+ and −/− mice were generated by breeding heterozygous mice. Ten to 12-week-old male C57/BL6 mice (Jackson Laboratory, Bar Harbor; ME, USA) were used for the experiments performed according to a protocol performed according to a protocol approved by the Institutional Animal Care and Use Committee of Ewha Womans University (EWHA IACUC 21-034-t). The mice were housed in a temperature-controlled room (20–22 °C) with alternating 12 h periods of light and dark. Mice were intraperitoneally injected with a single dose of cisplatin or saline. To increase the stability of cisplatin, 0.1 % Tween 80 was added to the saline. After the indicated times from injection, the mice were euthanized, and the kidneys and serum were collected for further analysis.

2.2. Histology and immunohistochemistry

Kidneys were fixed in 4 % paraformaldehyde, embedded in paraffin, and sectioned. Sections (4 μm thick) were then depleted of paraffin and subjected to hematoxylin and eosin (H&E) staining or immunohistochemical characterization using antibodies specific to anti-4HNE (JalCA, Tokyo, Japan) and 3-nitrotyrosine (3NT; Millipore, Darmstadt, Germany). Sections for immunohistochemistry were deparaffinized and immunolabeled with the corresponding antibodies. Visualization was performed using the peroxidase/DAB method. Stained sections were photographed using a microscope equipped with AxioCam software (Carl Zeiss, Jena, Germany).

2.3. Assessment of renal function

Blood was collected from the inferior vena cava and plasma was separated by centrifugation at 3000 rpm for 15 min at 4 °C. Plasma alanine aminotransferase (ALT) and aspartate transaminase (AST) concentrations were determined using the EnzyChromTM assay kits (BioAssay Systems, Hayward, CA, USA), according to the manufacturer's instructions.

2.4. Immunoblot analysis

The protein levels in the cells and mouse tissues were evaluated by immunoblot analysis. Cells and tissues were lysed with a cold lysis buffer (20 mM HEPES pH 7.0, 0.15 M NaCl, 10 % glycerol, 1 % Triton X-100, 1 mM EDTA, 1 mM EGTA, 10 mM β-phosphoglycerate, 1 mM Na3VO4, 5 mM NaF, 1 μg/mL aprotinin, 1 μg/mL leupeptin, and 100 μM phenylmethyl sulfonyl fluoride [PMSF]) using a polytron homogenizer or sonicator. The homogenates were centrifuged at 15,000 rpm, 4 °C for 15 min. After the protein present in the lysates were concentrated from supernatants using the Bradford assay (Bio-Rad, Hercules, CA, USA), the lysates were mixed with sample buffer (62.5 mM Tris-HCl pH 6.8, 10 % glycerol, 2 % sodium dodecyl sulfate, 0.0125 % bromophenol blue, and 2.5 % β-mercaptoethanol) and heated at 95 °C for 5 min. Proteins in sodium dodecyl sulfate (SDS) buffer (3 g/L Tris, 14.35 g/L glycine, and 1 g/L SDS) were separated by SDS-polyacrylamide gel electrophoresis (SDS-PAGE). The proteins were transferred onto an activated 0.45 μm pore size polyvinylidene difluoride (PVDF) membrane (Millipore, Darmstadt, Germany) using methanol with transfer buffer (3.03 g/L Tris, 14.17 g/L glycine, and 20 % methanol). The PVDF membrane was incubated with 5 % bovine serum albumin (BSA) in Tween-20 Tris-buffered saline at room temperature for 20 min using a rocker, followed by incubation at 4 °C overnight on a rocker with antibodies (1:2000 dilution). Cell or tissue lysates were fractionated by SDS-PAGE and the separated proteins were transferred to a PVDF membrane (Merck), which was then incubated with specific antibodies. Anti-actin, anti-LC3 (Sigma-Aldrich), anti-CuZnSOD, anti-MnSOD, anti-GAPDH, anti-Prx-SO_3 (AbFrontier), anti-Prx I to VI, anti-Srx [25,26], and anti-p62 antibodies were used as described previously [27]. Immune complexes were detected using horseradish peroxidase-conjugated secondary antibodies and enhanced with chemiluminescent reagents (AbFrontier). The abundance of target proteins was quantified by densitometric analysis of the immunoblots.

2.5. Cell culture

HepG2 cells, mProx24 cells, and MEFs were maintained under 5 % CO_2 at 37 °C in Dulbecco's modified Eagle's medium supplemented with 10 % fetal bovine serum, penicillin, and streptomycin. The cells were treated with various concentrations of cisplatin in dimethylformamide (DMF) for the indicated time periods. The cells were treated with 3-methyladenine, lactacystin, and MG132 for 3 h before cisplatin treatment.

2.6. Cell viability assay

Cell viability was measured by MTT assay. HepG2 cells were seeded in 96-well plates at a density of 4×10^4 cells/well, and MEFs were seeded at a density of 1×10^4 cells/well. On the next day, cells were treated with various concentrations of cisplatin in growth media for 24 h and then, cells were gently washed twice with growth medium and incubated with 0.5 mg/mL MTT (Sigma-Aldrich) at 37 °C for 1 h. The formazan crystals formed by active mitochondria were dissolved in dimethyl sulfoxide (DMSO), and the A_{540} of each well was measured using a spectrophotometer.

2.7. Subcellular fractionation

Mouse tissues were finely minced, homogenized using a Douncer homogenizer in isolation buffer (230 mM mannitol, 70 mM sucrose, 10 mM Tris-HCl pH 7.4, 1 mM EDTA, and 0.1 % BSA), and centrifuged at 1000×*g* for 10 min. The supernatant (PNS) was centrifuged at 12,000×*g* for 10 min. The mitochondrial pellet was washed twice with wash buffer (230 mM mannitol, 70 mM sucrose, 10 mM Tris-HCl, and pH 7.4) and the resulting supernatant was further centrifuged at 96,000×*g* for 1 h. The supernatant was collected as the cytosolic fraction and the microsomal pellet was dissolved in lysis buffer.

2.8. RT-PCR and quantitative real-time PCR

The samples were lysed with 1 mL of TRIzol (Invitrogen, Carlsbad, CA, USA) using a homogenizer on ice. Chloroform was added (200 μL) and vigorously vortexed for 15 s, followed by a 3 min rest to separate the phenol from lysate, then centrifuged at 12,000×*g*, 4 °C for 15 min. The lysates were separated into three layers. The aqueous top layer

containing RNA was transferred to another tube. Isopropanol was added (500 μL) and the tube was inverted gently four times and kept at −80 °C for 16 h for precipitation of the RNA. Subsequently, the frozen mixture in the tube was melted on ice, then centrifuged at 12,000×*g* and 4 °C for 10 min. The pellet was washed twice with 70 % ethanol in RNase-free water, centrifuged at 12,000×*g* and 4 °C for 10 min, and dried. The RNA pellet was then resuspended in RNase-free water. The RNA purity and concentration were determined using a NanoDrop ND-1000 spectrophotometer (Daemyung, Seoul, Republic of Korea). Total RNA was isolated from cultured cells using TRIzol reagent. Random hexamer primers were added at room temperature and complementary DNA (cDNA) was synthesized using the ABI cDNA Synthesis Kit (Applied Biosystems, Waltham, MA, USA). The resulting cDNA was subjected to real-time PCR using SYBR Green (PerkinElmer, Foster City, CA, USA) on an ABI PRISM 7700 system (PerkinElmer). Glyceraldehyde 3-phosphate dehydrogenase (GAPDH) was used as an internal control. Primer sequences for mouse cDNAs (forward and reverse) are listed in Table 1.

2.9. Statistical analysis

Western blot protein bands were quantified by densitometry using ImageJ software (IMAGEJ 1.50I, USA). All values are expressed as means ± standard error (S. E.). Statistical significance was analyzed by 2-factor ANOVA for multiple comparisons using GraphPad Prism software version 6 (GRAPHPAD, USA). Statistical significance was set at $p < 0.05$. significant.

3. Results

3.1. Cisplatin-induced nephrotoxicity and selective degradation of Prx I

To investigate the effects of cisplatin on antioxidant proteins in the kidney, 30 mg/kg cisplatin or saline was injected into C57/BL6 mice (n = 4 per group). Mice were euthanized after 3 d, and kidney and serum samples were collected. Severe kidney damage was induced following the administration of cisplatin, as evidenced by significant cast formation and dilated tubular cells in cisplatin-treated kidneys compared with sham kidneys (Fig. 1A). Additionally, kidney damage indicators, such as blood urea nitrogen (BUN) and serum creatinine (SCr) concentrations, were significantly elevated and body weight was decreased in cisplatin-treated mice (Fig. 1B). To assess the changes in antioxidant proteins, kidney lysates were subjected to immunoblot analysis with antibodies against various antioxidant proteins (Fig. 1C and D). Among these, only Prx I protein levels showed a significant decrease when normalized to GAPDH levels. To determine whether the decrease in Prx I protein levels was due to degradation or reduced protein synthesis, Prx I mRNA levels were measured using quantitative PCR. Despite the decrease in Prx I protein levels, Prx I mRNA levels increased (Fig. 1E), indicating that Prx I was selectively degraded in response to cisplatin-induced kidney damage.

These results suggest that cisplatin induces significant nephrotoxicity, characterized by structural and functional kidney damage, and selectively degrades Prx I despite increased Prx I mRNA levels, thereby highlighting a targeted response in the antioxidant defense mechanism.

3.2. Cisplatin-induced ER stress and Prx I degradation over time in mouse kidneys

To further investigate the degradation of Prx I over time-course, 20 mg/kg cisplatin was administered to C57/BL6 mice after which they were euthanized after the indicated times. The damaged kidneys were collected and analyzed (Fig. 2). Despite the relatively slow decrease in Prx I protein levels, a significant reduction was observed 72 h after cisplatin injection. The initial increase in Prx I mRNA levels, followed by a decrease in protein levels, indicated that Prx I was selectively degraded in response to cisplatin-induced stress despite an increase in transcription (Fig. 2A and B). To determine whether cisplatin-induced nephrotoxicity is closely related to increased levels of ROS, we evaluated the oxidative stress response by measuring the mRNA levels of antioxidant response elements such as Nrf2, HO-1, and Srx. The results showed a time-dependent increase in these mRNA levels, with significant elevations observed 48 and 72 h after cisplatin injection. This suggests that kidneys upregulate antioxidant defense mechanisms in response to increased oxidative stress (Fig. 2B).

Cisplatin accumulates in the proximal tubular epithelial cells and induces ROS generation, leading to oxidative stress and cellular apoptosis [28–30]. Prx I plays a role in scavenging ROS on the ER surface; however, following cisplatin treatment, Prx I protein levels decrease, impairing the ROS removal capacity. Consequently, we confirmed a reduction in Prx I expression by isolating the ER (Fig. 2C). Upon further analysis, Prx I degradation was found to occur more rapidly in the ER fraction compared to the cytosolic fraction after cisplatin treatment, indicating that the ER is a key site of oxidative damage and that ER-localized Prx I is particularly susceptible to degradation under these conditions (Fig. 2D). Additionally, in cisplatin-treated kidneys, the ER stress markers, ATF4 and TRB3, were induced in a time-dependent manner (Fig. 2E), which was consistent with previous studies indicating that ER stress played a crucial role in cisplatin-induced nephrotoxicity [8,31]. The BUN and serum creatinine levels also increased sharply after 72 h (data not shown), indicating that

Table 1
Primers used for real-time PCR.

Target Gene	Forward primer (5' - 3')	Reverse primer (5' - 3')
GAPDH	AGAACATCATCCCTGCATCC	GGTCCTCAGTGTAGCCCAAG
Prx I	ACCATTGCTCAGGATTATGGA	CAACGGGAACGACGTTTATTG
Prx II	CAATGTGGATGACAGCAAGG	CCCTTCAGAGAGTGGAGGAA
Prx III	GGAAGAAACACTCCGTTTGG	GTTGGACTTGGCTTGATCGT
Prx IV	CAGCACCTTATTGGGAAGGA	GCGATGATTTCAGTTGGACAC
Prx V	GGCATTTACACCTGGCTGTT	CGACGATTCCCAAAGAGAGA
Prx VI	GTAGTGTCAGTGTGGGCTCT	GAGGTACATGCGCACTCTTG
Nrf-2	CTCTCTGAACTCCTGGACGG	GGGTCTCCGTAAATGGAAG
Srx	GGAAGGAAGAAAGGAGATGG	AGAGTTCAGGCTATGGGGAT
HO-1	CACGCATATACCCGCTACCT	CCAGAGTGTTCATTCGAGCA
CYP2E1	CGTTGCCTTGCTTGTCTGGA	AAGAAAGGAATTGGGAAAGGTCC
p62	CCGCCGCTTCAGCTTCTGCT	GTTCCCGCCGGCACTCCTTC
ATF4	ATGGCCGGCTATGGATGAT	CGAAGTCAAACTCTTTCAGATCCATT
TRB3	CTCTGAGGCTCCAGGACAAG	GGCTCAGGCTCATCTCTCAC
XBP1s	GAGTCCGCAGCAGGTG	GTGTCAGAGTCCATGGGA
Edem 1	GCAATGAAGGAGAAGGAGACCC	TAGAAGGCGTGTAGGCAGATGG
Grp78	GGTGCAGCAGGACATCAAGTT	CCCACCTCCAATATCAACTTGA
IL-1b	TCGTGCTGTCGGACCCATAT	GTCGTTGCTTGGTTCTCCTTGT
TNF-a	GCCACCACGCTCTTCTG	GGTGTGGGTGAGGAGCA

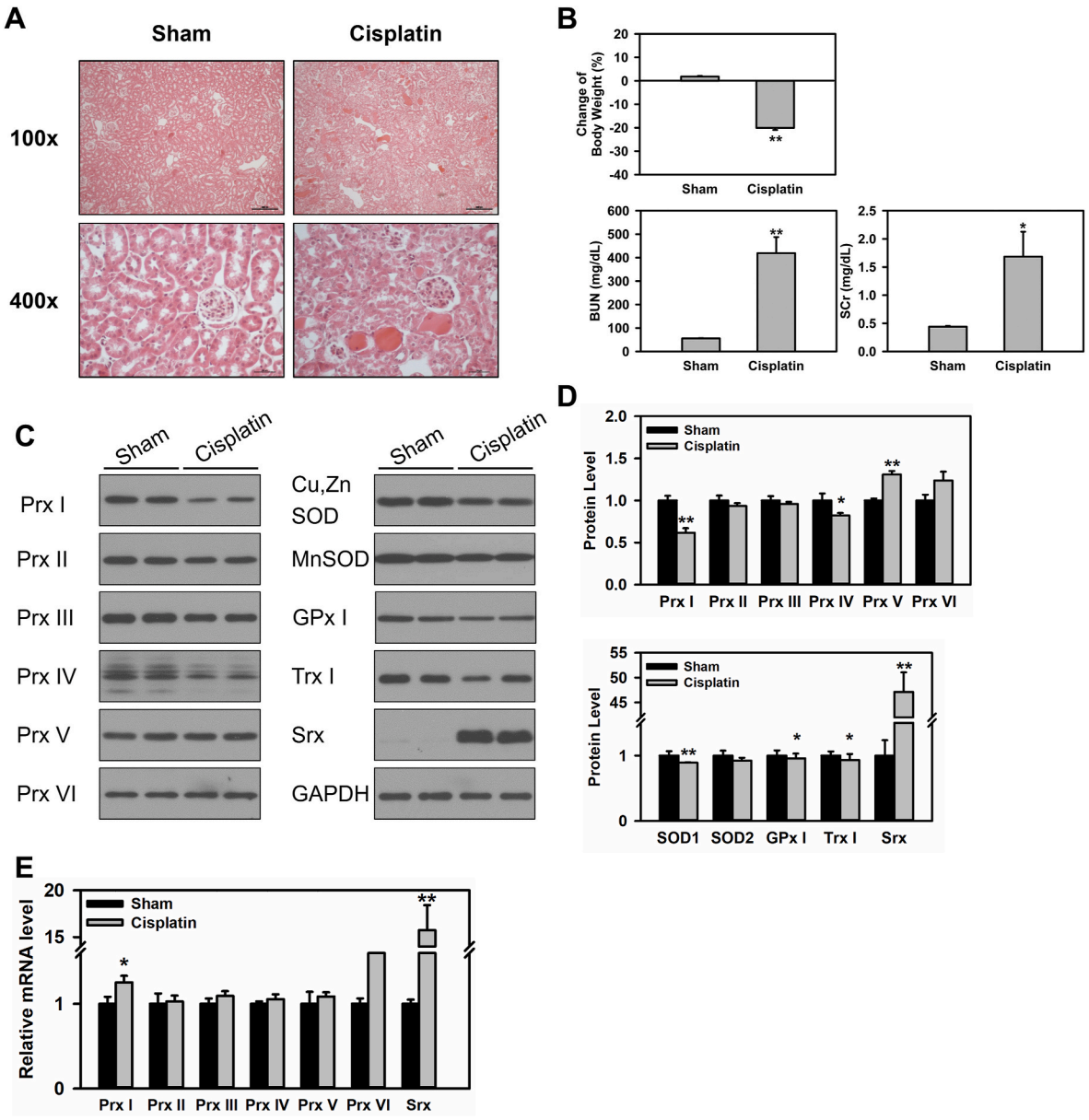


Fig. 1. Effect of cisplatin on the kidney of C57/BL6 mice and selective decrease of Prx I in cisplatin-treated kidney.
Male C57/BL6 mice were treated with 30 mg/kg cisplatin via a single intraperitoneal injection of cisplatin and euthanized after 72 h (n = 4, each). Serum and kidney samples were obtained for further analysis. (A) Kidneys were fixed overnight in 4 % paraformaldehyde and embedded in paraffin blocks. Kidney sections (4 μm thick) from sham and cisplatin-treated mice were subjected to H&E staining. Original magnification, 100× and 400x. (B) Body weight changes were measured before euthanasia. Indicators of renal function in the sera of sham and cisplatin-treated mice were measured. BUN, blood urea nitrogen; SCr, serum creatinine (C) mice treated with 30 mg/kg cisplatin for 72 h (n = 4, each). Kidneys of sham and cisplatin-treated mice were lysed and subjected to immunoblot analysis. Antibodies against various antioxidant proteins have also been developed. (D) Densitometry analysis of (C). Each blot was normalized to GAPDH. (E) mRNA levels of antioxidant proteins in sham and cisplatin-treated kidneys were measured using quantitative PCR. mRNA levels were normalized to those of GAPDH. Data in (B), (D) and (E) are presented as the means ± SE. *$p < 0.05$, **$p < 0.01$.

kidney function was impaired in the late stages of cisplatin damage.

These findings suggest that Prx I is selectively degraded during the late stages of cisplatin-induced kidney damage and that this process is closely associated with both the oxidative stress and ER stress pathways.

3.3. *Selective degradation of Prx I through autophagy in cisplatin-induced kidneys*

To elucidate the mechanism of Prx I degradation, we investigated the involvement of autophagic and proteasomal degradation pathways. The treatment of mProx24 cells with cisplatin initiated PrxI degradation after 18 h (Fig. 3A). Under these conditions, a significant increase in LC3-II and decrease in p62 levels were observed, indicating the formation of autophagosomes. Therefore, we conducted additional experiments using autophagy inhibitors and proteasomes. An experiment using 3-methyladenine (3-MA), a known autophagy inhibitor, showed that 3-MA inhibited cisplatin-induced Prx I degradation (Fig. 3B). This suggests that Prx I was degraded via cisplatin-mediated autophagic degradation. In contrast, the proteasome inhibitors lactacystin and MG132 did not block the degradation of Prx I but rather accelerated it (Fig. 3C and D). This acceleration of Prx I degradation could be due to increased autophagy as a compensation for the inhibition of proteasomal degradation [32].

These results strongly indicate that autophagy plays a critical role in

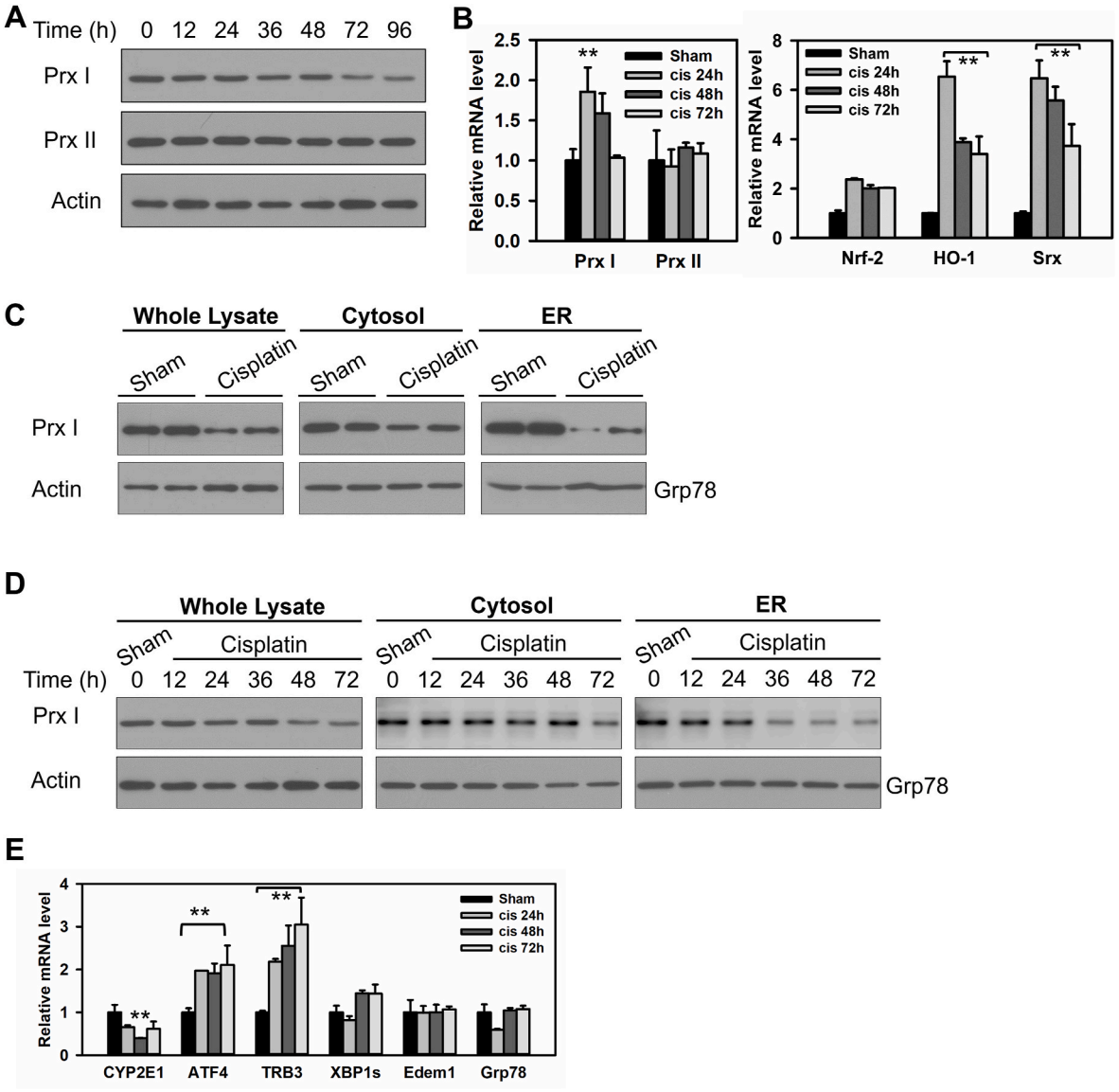


Fig. 2. Time-dependent effects of cisplatin on protein and mRNA expression levels in the kidneys of C57/BL6 mice.
(A) C57/BL6 mice were injected 20 mg/kg of cisplatin and euthanized 12, 24, 36, 48, 72, and 96 h after injection. Kidney lysates were subjected to immunoblot analysis. Data are representative of three independent experiments. (B) The mRNA levels of sham and cisplatin-treated kidney were measured by quantitative PCR and normalized by GAPDH mRNA. (C, D) Whole lysates, cytosolic, and ER fractions obtained after subcellular fractionation of kidney homogenates were then subjected to immunoblot analysis with antibodies to indicated proteins. (E) The mRNA levels of sham and cisplatin-treated kidney were measured by quantitative PCR and normalized by GAPDH mRNA. Data are represented as mean ± SE. **$p < 0.01$.

the degradation of Prx I. Specifically, the autophagic pathway activated by cisplatin treatment appears to be the primary mechanism for the selective degradation of Prx I. Inhibition of Prx I degradation by the autophagy inhibitor 3-MA provides compelling evidence that autophagy is the major pathway for Prx I degradation. Furthermore, the acceleration of Prx I degradation by proteasome inhibitors suggests that autophagy may act as a compensatory mechanism in response to inhibition of proteasomal degradation.

To further study the role of autophagy in cisplatin-induced Prx I degradation, we used autophagy-defective ATG7 knockout (KO) MEF. In ATG7 wild-type (WT) MEF, cisplatin induces Prx I degradation and autophagy. In contrast, the absence of ATG7 completely blocked the degradation of Prx I by cisplatin (Fig. 3E and F), suggesting that autophagy is the major pathway for Prx I degradation.

In conclusion, Prx I degradation primarily occurred via the autophagic pathway triggered by cisplatin treatment. The results obtained with proteasome inhibitors imply an interaction between the autophagic and proteasomal degradation pathways, with autophagy playing a crucial role in Prx I degradation. These findings enhance our understanding of the Prx I degradation mechanism and could contribute to the development of new therapeutic strategies by modulating autophagic and proteasomal pathways in future research.

3.4. *Mechanism of cisplatin-induced Prx I degradation in CYP2E1 overexpressing cells*

We hypothesized that the selective degradation of Prx I compared to other Prxs was due to its unique localization. Prx I is the only Prx protein that localizes to the ER surface [24]. Moreover, the ER membrane is considered the source of phagophores that initiate macroautophagy [33]. Therefore, Prx I on the ER surface is degraded by autophagy stimulated by cisplatin-induced ER stress.

To test this hypothesis, we used the HepG2 cell line overexpressing CYP2E1, which generates more ROS on the ER surface and induces ER

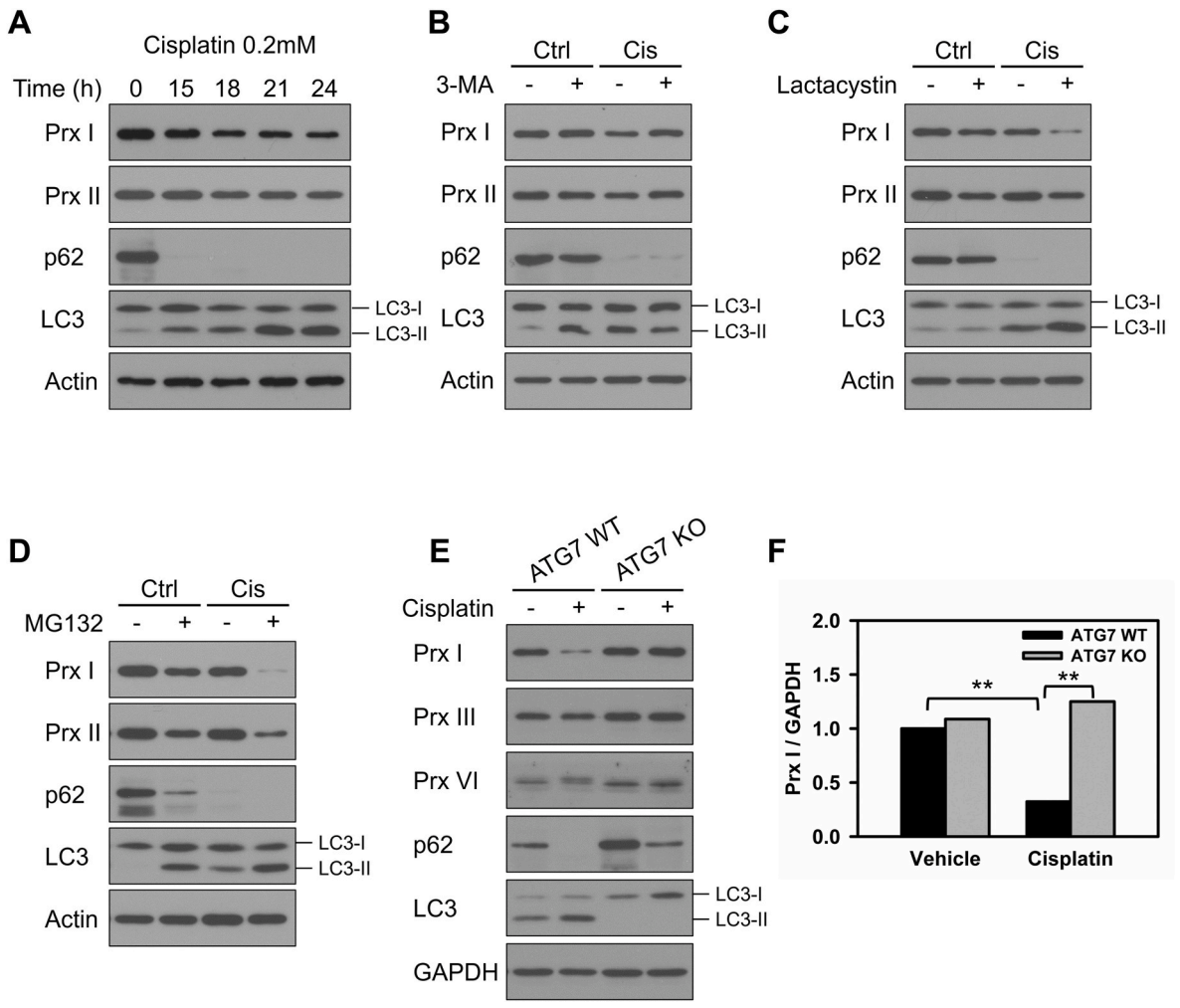


Fig. 3. Inhibition of Prx I degradation by autophagy inhibitors in mouse proximal tubular cells and cisplatin-induced Prx I degradation in autophagy-deficient ATG7 KO MEF cells.
(A) mProx24 were treated with 0.2 mM of cisplatin dissolved in DMF in growth media for 0, 15, 18, 21, 24 h, and harvested. The cell lysates were subjected to immunoblot analysis. (B) 5 mM of 3-MA or (C) 10 μM of lactacystin or (D) 10 μM of MG132 or each vehicle was pre-treated in growth media. After 3 h, 0.2 mM of cisplatin or DMF alone was added. Cells were harvested after 18 h from cisplatin treatment. The cell lysates were subjected to immunoblot analysis. (E) ATG7 WT and ATG7 KO MEFs were treated with 0.15 mM of cisplatin or DMF alone for 16 h in growth media and harvested. Cell lysates were subjected to immunoblot analysis. (F) Densitometric analysis of (E). Intensity of Prx I was normalized by that of GAPDH. Data in (F) are means ± SE. **$p < 0.01$.

stress upon cisplatin treatment [20,34]. Prx I degradation occurred much faster in CYP2E1 overexpressing (E47) cells than in control (C34) cells, whereas other cytosolic Prxs showed no change (Fig. 4A). In addition, E47 cells were more vulnerable to cisplatin-induced cell death than C34 cells (Fig. 4B). These data suggest that Prx I degradation is related to ER stress.

Since cisplatin-induced degradation of Prx I is mediated by autophagy in mouse proximal tubular cells and MEFs, we also tested whether autophagy mediates Prx I degradation in E47 cells. The autophagy inhibitor 3-MA partially blocked cisplatin-induced Prx I degradation (Fig. 4C and D), indicating that Prx I degradation is mediated by autophagy. No change was observed in Prx I mRNA levels in cisplatin-treated cells pretreated with vehicle or 3-MA (Fig. 4E). The protein level of p62 significantly decreased in cisplatin-treated cells, whereas p62 was increased *in vivo* following cisplatin treatment. This discrepancy was due to the decrease of p62 mRNA levels observed *in vitro*, but not *in vivo* (Fig. 4C–E).

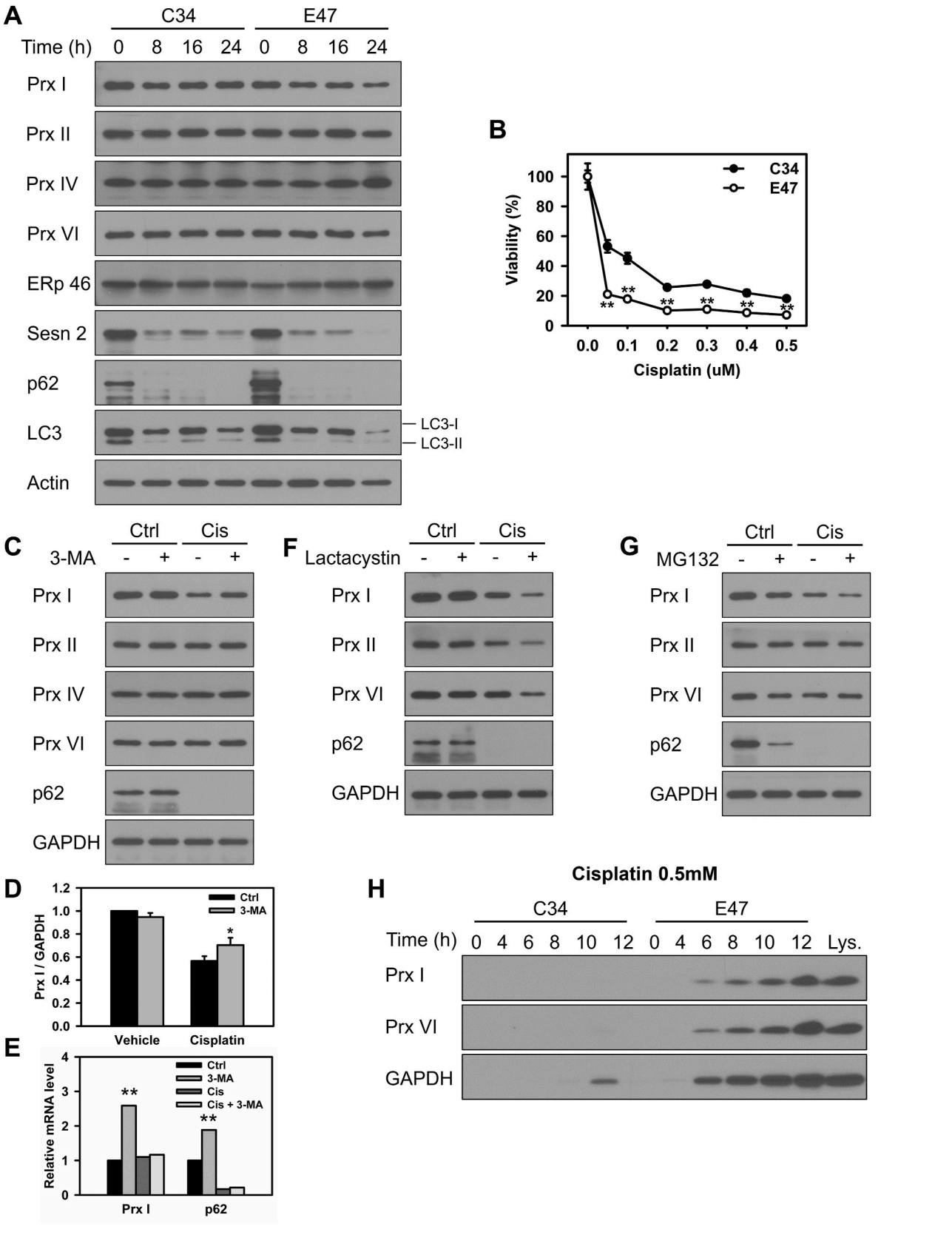
To exclude proteasomal degradation, We used lactacystin and MG132 to cisplatin treated E47 cells. None of the inhibitors blocked Prx I degradation (Fig. 4F and G), which was consistent with the results for mProx24 cells and MEFs.

We also investigated whether the decrease in Prx I was due to degradation or secretion into the medium, as Prx I has been reported to be released into the serum or extracellular space [35,36]. We treated C34 and E47 cells with cisplatin in serum-free media to eliminate Prx I present in fetal bovine serum. Media samples (200 μL) were collected at the indicated times and subjected to immunoblot analysis. Prx I, Prx VI, and GAPDH were gradually detected in the cisplatin-treated E47 cells (Fig. 4H), although Prx VI and GAPDH levels were not decreased following cisplatin treatment. The presence of these proteins in the medium was attributed to cell lysis during cell death, rather than active secretion.

Collectively, ROS produced by CYP2E1 on the ER surface induce ER stress, which leads to autophagy and subsequent degradation of Prx I in CYP2E1 overexpressing cells.

3.5. *Impact of Prx I-deficiency on cisplatin-induced renal injury and stress response pathways*

Prx I removes ROS produced by CYP2E1 from the ER surface because of its proximity to CYP2E1 [24]. Since ER stress plays a crucial role in autophagy during cisplatin treatment, we investigated the role of Prx I in



(caption on next page)

Fig. 4. Effect of CYP2E1 overexpression, autophagy inhibition, and proteasomal degradation or secretion on Prx I degradation by cisplatin.
(A) CYP2E1 overexpressing HepG2 cells (E47) and control HepG2 cells (C34) were treated with 0.5 mM of cisplatin in growth media for 0, 8, 16, 24 h and harvested. Cell lysates were subjected to immunoblot analysis. (B) C34 and E47 cells were treated with indicated concentrations of cisplatin for 24 h. Cells were incubated with 0.5 mg/mL of MTT for an hour at 37 °C. The formazan crystals formed by active mitochondria were dissolved in DMSO and A_{540} for each well was measured with spectrophotometer. Cell viability was calculated by the absorbance. Data are represented as mean ± SE for three independent experiments. **$p < 0.01$ vs C34 (C) E47 cells were pre-treated with 5 mM of 3-MA or vehicle in growth media. After 3 h, 0.5 mM of cisplatin or DMF alone was treated for 16 h and cells were harvested. Cell lysates were subjected to immunoblot analysis. Data are representative of five independent experiments. (D) Densitometric analysis of (C). Intensity of Prx I was normalized by that of GAPDH. Data are represented as mean ± SE for five independent experiments. *$p < 0.05$. (E) mRNA levels of Prx I and p62 were measured with quantitative PCR. Each mRNA was normalized by actin mRNA. (F) E47 cells were pre-treated with 10 μM of lactacystin or (G) 10 μM of MG132 or vehicle in growth media. After 3 h, 0.5 mM of cisplatin or DMF only was treated and cells were harvested. Cell lysates were subjected to immunoblot analysis. (H) C34 and E47 cells were treated with 0.5 mM of cisplatin in serum-free media. Media was collected after 0, 4, 6, 8, 10, 12 h and the collected media were added immediately with SDS sample buffer and boiled. The 40 μL of each sample was subjected to immunoblot analysis. 2 μg of E47 cell lysate (Lys) was loaded on the same SDS-PAGE as a control. Data are represented as mean ± SE for three independent experiments. **$p < 0.01$.

ER stress by injecting cisplatin into Prx I KO mice.

Histological analysis showed that Prx I KO mice were more damaged by cisplatin. Cisplatin-treated Prx I KO mice showed increased cast formation, necrosis, and desquamation in proximal tubules (Fig. 5A). Renal function was measured in the cisplatin-treated KO mice (Fig. 5B). The BUN level in Prx I KO mice increased to 372.1 ± 69.6 mg/dL, whereas it was only 263.0 ± 45.5 mg/dL in Prx I WT mice. The SCr level in Prx I KO mice was 1.47 ± 0.28 mg/dL, compared to 0.90 ± 0.24 mg/dL in Prx I WT mice. Both BUN and SCr levels indicated that renal function was significantly impaired in cisplatin-treated Prx I KO mice.

Immunohistochemical analysis was performed using antibodies against the damage markers. 3-Nitrotyrosine (3-NT) was used as a biomarker for RNS formation, and 4-hydroxynonenal (4-HNE) protein adducts were used as markers of oxidative stress. Both 3-NT and 4-HNE levels were significantly higher in the kidneys of cisplatin-treated Prx I KO mice than in wild-type mice (Fig. 5C and D). These data suggest that Prx I KO mice are more susceptible to cisplatin-induced kidney damage than wild-type mice.

Protein levels were determined by immunoblot analysis (Fig. 6A). Although mRNA levels increased in Prx I KO mice, protein levels did not show significant changes, suggesting that changes in protein levels may occur at later stages of cisplatin-induced damage.

Additionally, mRNA levels of oxidative damage markers were measured (Fig. 6B). IL-1β and TNF-α were significantly increased in Prx I KO mice, indicating increased inflammation. Levels of the redox-sensitive transcription factor Nrf-2 and its target Srx were also elevated in Prx I KO mice. Furthermore, ATF4, TRB3, and XBP1s were more induced to a greater extent in Prx I KO mice, indicating increased ER stress. These data suggest that Prx I deficiency exacerbates cisplatin-induced damage.

4. Discussion

Cisplatin is a widely used antineoplastic drug for the treatment of a broad range of tumors, and its primary mechanism of action has historically been believed to be DNA damage [1,5]. Although cisplatin primarily targets DNA, only a fraction of intracellular cisplatin binds directly to nuclear DNA. A significant proportion of cisplatin interacts with various cellular components including proteins, lipids, and RNA, contributing to its broad cytotoxic effects. Moreover, the relationship between cisplatin sensitivity and p53 status in tumor cells remains unclear [8,37,38].

Recent studies have shown that cisplatin induces apoptosis primarily through the mitochondrial (intrinsic) pathway, which involves interactions between the Bcl-2 family proteins and mitochondrial dysfunction [39–41]. Upon entering the cell, cisplatin accumulates in the mitochondria where it generates mitochondrial reactive oxygen species, leading to oxidative stress and damage to the mitochondrial membrane. This loss of mitochondrial membrane potential is a critical event that facilitates the release of cytochrome *c*, which in turn activates Apaf-1 to form an apoptosome complex, triggering the activation of caspase-9 and caspase-3, thereby promoting cell death via the apoptotic pathway [42,43]. In addition to its role in apoptosis, recent evidence has suggested that ER stress is a significant contributor to cisplatin-induced cytotoxicity. Although many studies have focused on the relationship between ER stress and apoptosis, growing evidence indicates that ER stress may also enhance autophagy, a cellular response that can act as a survival mechanism in some contexts [6–9]. Interestingly, autophagy has been observed following cisplatin treatment, both *in vivo* and *in vitro*, suggesting that cisplatin-induced cytotoxicity involves a complex interplay between apoptosis and autophagy, with the balance between these processes potentially influencing the overall treatment [11–14]. This dual pathway, apoptosis via mitochondrial dysfunction and autophagy enhancement through ER stress, highlights the complexity of the cisplatin-induced cytotoxicity and underscores the need for further investigation into how these mechanisms could be modulated to improve therapeutic outcomes and minimize resistance [43,44].

Building on this understanding, in this study, we focused specifically on cisplatin-induced ER stress and autophagy. Since Prx I is the only peroxiredoxin residing on the ER surface that reduces ROS production on the ER membrane [24], we investigated the role of Prx I in cisplatin-induced cytotoxicity. We found that Prx I expression was significantly decreased in cisplatin-treated kidneys, whereas other antioxidant proteins remained unchanged (Fig. 1). The mRNA level of Prx I increased slightly, possibly through the Nrf-2 pathway [39], suggesting that the decrease in Prx I was due to protein degradation.

Prx I degradation was detected at the late stage of kidney damage, when renal function was severely impaired (Fig. 2). ER stress marker proteins involved in the PERK pathway, such as ATF4 and its downstream target TRB3, were induced immediately after cisplatin injection and persisted until renal function was compromised. Additionally, the increase in LC3-II levels indicated that autophagy was induced in cisplatin-treated kidneys, which was consistent with previous studies on the induction of autophagy by cisplatin [11].

The mechanism of Prx I degradation was investigated *in vitro* (Fig. 3). In the mouse proximal tubular cell line mProx24, cisplatin-induced Prx I degradation was blocked by 3-MA, an autophagy inhibitor, suggesting that Prx I was degraded via autophagy. Lactacystin and MG132 did not block Prx I degradation, possibly because these proteasome inhibitors enhanced autophagy [32]. Moreover, no cisplatin-induced degradation of Prx I was detected in autophagy-deficient ATG7 KO MEFs, confirming that Prx I is degraded through autophagy. The unique localization of Prx I to the ER surface likely accounts for its selective degradation. The ER membrane is believed to be a source of phagophores that initiate macroautophagy [33]. Therefore, we hypothesized that autophagy is induced by ER stress in cisplatin-induced cytotoxicity and that Prx I is degraded because it is associated with the phagophore.

To our knowledge, this is the first study to demonstrate that cisplatin-induced nephrotoxicity leads to the reduction of Prx I protein and that Prx I in the ER is selectively degraded by autophagy. This novel finding significantly advances our understanding of the molecular mechanisms underlying cisplatin-induced kidney damage and identifies Prx I as a key regulator of oxidative stress in this context. The identification of Prx I as a target of autophagic degradation during cisplatin-induced

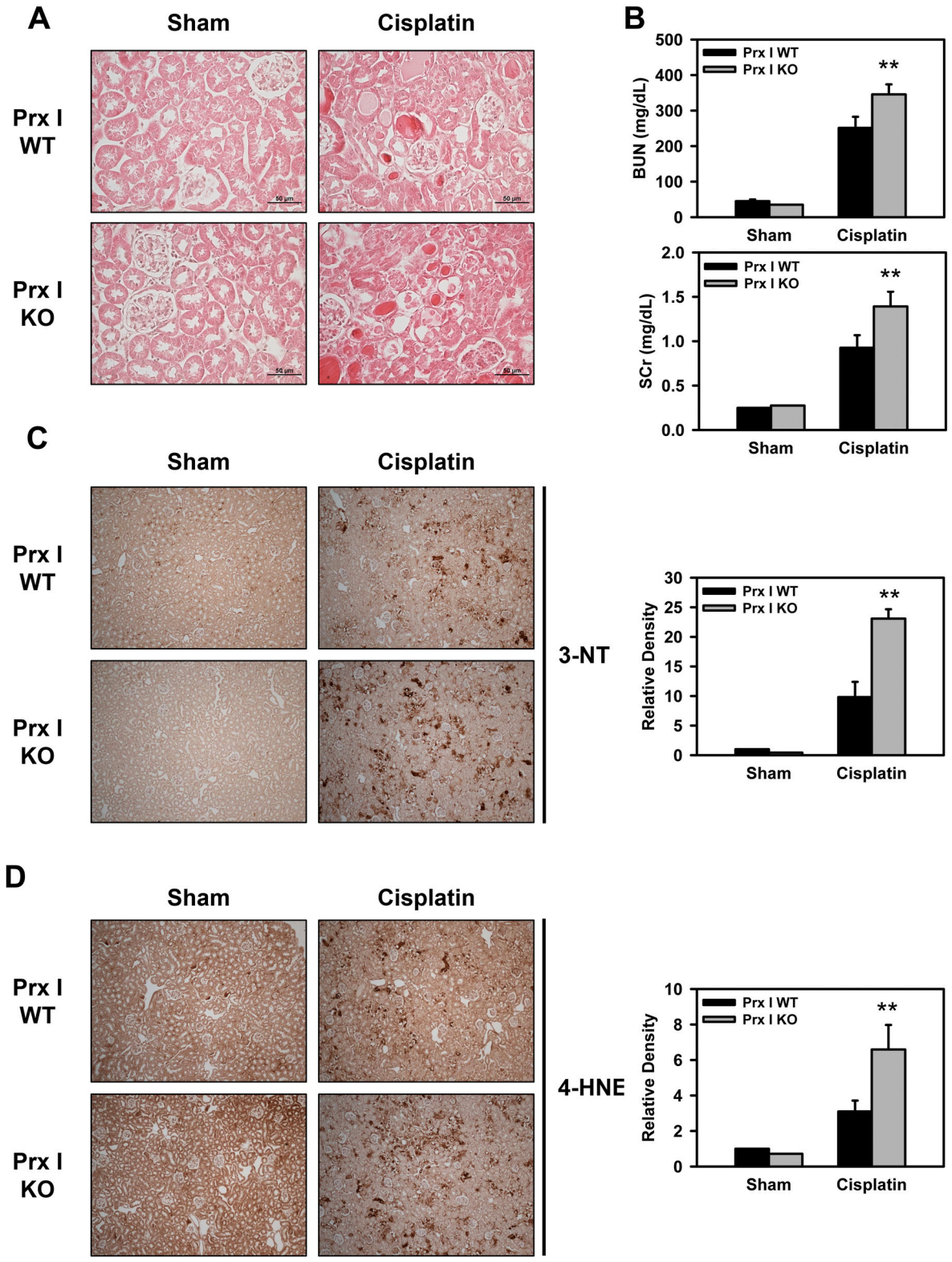


Fig. 5. Effect of Prx I ablation on oxidative kidney damage induced by cisplatin.
Male Prx I WT and Prx I KO mice were treated with 20 mg/kg cisplatin via a single intraperitoneal injection and sacrificed after 72 h. Serum and kidney samples were collected for further analysis. (A) Kidneys were fixed overnight in 4 % paraformaldehyde and embedded in paraffin blocks. Kidney sections (4 μm thick) from Prx I WT and Prx I KO mice that had been injected with cisplatin or saline were subjected to H&E staining. Original magnification, 400×. (B) Indicators of renal function in the sera of sham and cisplatin-treated mice were measured. BUN, blood urea nitrogen; SCr, serum creatinine (C, D) Kidney sections were subjected to immunohistochemical analysis with antibodies to (C) 3-NT or to (D) 4-HNE as described in materials and methods. Densitometric analysis of each section was performed using the ImageJ software (right). Original magnification, 100×. Data are represented as mean ± SE. **$p < 0.01$.

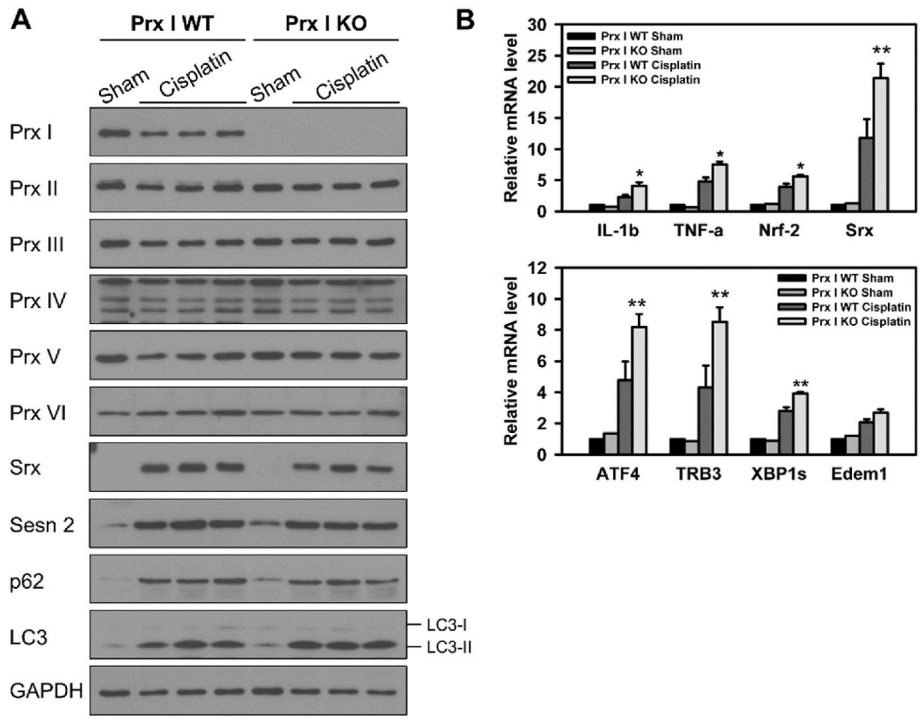


Fig. 6. Effects of Prx I ablation on gene expression, and expression of Prxs, Srx, and autophagy-related proteins in cisplatin-treated kidneys of Prx I WT and KO Mice. Male Prx I WT and Prx I KO mice were treated with 30 mg/kg cisplatin via a single intraperitoneal injection and euthanized after 72 h. The kidney samples were obtained for further analyses. (A) Lysates from each kidney were subjected to immunoblotting. The corresponding antibodies were used. (B) The mRNA levels in the kidneys were measured using quantitative PCR. Each mRNA was normalized to GAPDH mRNA. Data in (B) represent the mean ± SE. *p < 0.05, **p < 0.01.

nephrotoxicity not only provides new insights into the cellular responses to this chemotherapeutic agent but also highlights potential avenues for therapeutic intervention.

To study the effect of ER stress on cisplatin-induced Prx I degradation, ER stress was induced in response to cisplatin (Fig. 4). CYP2E1 localizes in the ER membrane and produces ROS on the ER surface [24, 45]. According to Baliga et al., CYP2E1 is involved in cisplatin-induced cytotoxicity by increasing ROS production *in vivo* [20] and the increased ROS induce ER stress [7]. Therefore, We used CYP2E1 overexpressing HepG2 cells (E47) to increase ROS production and ER stress after cisplatin treatment. E47 cells showed accelerated Prx I degradation and decreased viability in response to cisplatin compared to control cells (C34), indicating that increased ER stress boosts Prx I degradation and cell death. We also confirmed that cisplatin-induced Prx I degradation in E47 cells was mediated by autophagy but not by proteasomes or secretion.

Moreover, cisplatin-induced ER stress enhanced autophagy, resulting in the degradation of Prx I. Interestingly, the levels of other ER lumen proteins, such as Prx IV and ERp46, did not change, implying that only ER membrane-resident proteins were degraded through autophagy. Although the precise mechanism underlying Prx I degradation remains unclear, we attempted to elucidate the role of Prx I in cisplatin-induced cytotoxicity. Recent studies have shown that Prx I is localized to the ER surface and removes ROS produced by CYP2E1 in ethanol-fed mice because of its proximity [24]. Since CYP2E1 is also an important cause of ROS and ER stress in cisplatin-induced cytotoxicity and Prx I has a protective effect against cisplatin cytotoxicity [23], we focused on the role of Prx I as a peroxidase to reduce ROS on the ER surface. Prx I KO mice were more sensitive to cisplatin-induced nephrotoxicity (Fig. 5). Prx I deficiency augments kidney dysfunction and increases ER stress. These results showed that Prx I protects against cisplatin-induced nephrotoxicity by removing ROS produced on the ER surface, consequently decreasing ER stress.

In conclusion, our results suggest that Prx I is degraded by ER stress-induced autophagy during cisplatin-induced nephrotoxocity because of its localization to the ER membrane surface. Furthermore, Prx I plays a protective role by removing the ROS produced on the ER membrane, which induces ER stress (Fig. 7). Ironically, while Prx I provides protection against cisplatin-induced damage, it is degraded by cisplatin, further augmenting the damage. We suggest that Prx I is degraded after autophagosomes to which Prx I is attached are lysed by fusion with lysosomes, and that its protective effect is mediated by decreasing ER stress by removing ROS at the early stage of cisplatin-induced

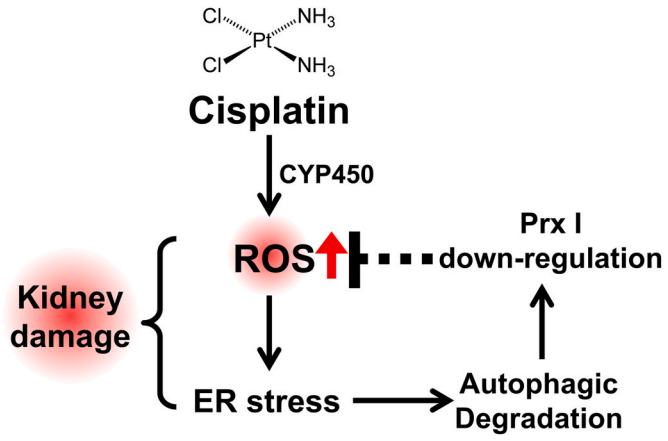


Fig. 7. Model for protective effect of Prx I and its degradation in the kidney of cisplatin-injected mice.
Cisplatin induces ER stress through two pathways: increasing misfolded proteins and the unfolded protein response, and by increasing ROS through CYP2E1 toward the ER surface. Prx I, which resides on the ER surface, removes ROS generated by CYP2E1. Therefore, Prx I exerts a protective effect by reducing cisplatin-induced ER stress. Endoplasmic reticulum (ER) stress initiates autophagy and phagophores are formed from the ER membrane. Prx I is involved in phagophores and is removed by autophagic degradation.

cytotoxicity. Although the mechanism underlying Prx I involvement in autophagy requires further investigation, understanding and potentially manipulating the autophagic degradation of Prx I could pave the way for new therapeutic approaches that enhance the efficacy of cisplatin while reducing its renal toxicity.

Institutional review board statement

All animal experiments were performed according to the protocol (EWHA IACUC 21-034-t) approved by the Institutional Animal Care and Use Committee of Ewha Womans University.

CRediT authorship contribution statement

Jiyoung Park: Investigation. **Juhyun Sim:** Investigation. **Ho Jin Yi:** Investigation. **Sue Goo Rhee:** Conceptualization. **Hyun Ae Woo:** Writing – review & editing, Supervision, Funding acquisition, Conceptualization.

Declaration of competing interest

The authors declare that they have no known competing financial interests or personal relationships that could have appeared to influence the work reported in this paper. This research was conducted in the absence of any commercial or financial relationships that could be construed as a potential conflict of interest.

Acknowledgements

We thank Cederbaum, A.I. for the HepG2 C34 and E47 cells and I. H. LEE for *Atg7*$^{+/+}$ and *Atg7*$^{-/-}$ MEFs. This research was funded by grants from the National Research Foundation of Korea (2021R1A2C2095037, 2022K2A9A1A06093625 H.A.W. was supported by a Mid-career Research Grant and 2021R1C1C2006086 _Sejong Science Fellowship_SSF (J.P was supported to SSF)).

References

[1] R.P. Miller, R.K. Tadagavadi, G. Ramesh, W.B. Reeves, Mechanisms of cisplatin nephrotoxicity, Toxins 2 (11) (2010) 2490–2518.
[2] S.M. Sancho-Martinez, L. Prieto-Garcia, M. Prieto, J.M. Lopez-Novoa, F.J. Lopez-Hernandez, Subcellular targets of cisplatin cytotoxicity: an integrated view, Pharmacol. Ther. 136 (1) (2012) 35–55.
[3] J.T. Hartmann, H.P. Lipp, Toxicity of platinum compounds, Expet Opin. Pharmacother. 4 (6) (2003) 889–901.
[4] I. Arany, R.L. Safirstein, Cisplatin nephrotoxicity, Semin. Nephrol. 23 (5) (2003) 460–464.
[5] D. Wang, S.J. Lippard, Cellular processing of platinum anticancer drugs, Nat. Rev. Drug Discov. 4 (4) (2005) 307–320.
[6] B.S. Cummings, J. McHowat, R.G. Schnellmann, Role of an endoplasmic reticulum Ca2+-independent phospholipase A2 in cisplatin-induced renal cell apoptosis, J. Pharmacol. Exp. Therapeut. 308 (3) (2004) 921–928.
[7] H. Liu, R. Baliga, Endoplasmic reticulum stress-associated caspase 12 mediates cisplatin-induced LLC-PK1 cell apoptosis, J. Am. Soc. Nephrol. 16 (7) (2005) 1985–1992.
[8] A. Mandic, J. Hansson, S. Linder, M.C. Shoshan, Cisplatin induces endoplasmic reticulum stress and nucleus-independent apoptotic signaling, J. Biol. Chem. 278 (11) (2003) 9100–9106.
[9] Y. Xu, et al., Inhibition of autophagy enhances cisplatin cytotoxicity through endoplasmic reticulum stress in human cervical cancer cells, Cancer Lett. 314 (2) (2012) 232–243.
[10] W.X. Ding, X.M. Yin, Sorting, recognition and activation of the misfolded protein degradation pathways through macroautophagy and the proteasome, Autophagy 4 (2) (2008) 141–150.
[11] S. Periyasamy-Thandavan, et al., Autophagy is cytoprotective during cisplatin injury of renal proximal tubular cells, Kidney Int. 74 (5) (2008) 631–640.
[12] G.P. Kaushal, V. Kaushal, C. Herzog, C. Yang, Autophagy delays apoptosis in renal tubular epithelial cells in cisplatin cytotoxicity, Autophagy 4 (5) (2008) 710–712.
[13] D. Liu, Y. Yang, Q. Liu, J. Wang, Inhibition of autophagy by 3-MA potentiates cisplatin-induced apoptosis in esophageal squamous cell carcinoma cells, Med. Oncol. 28 (1) (2011) 105–111.
[14] C. Yang, V. Kaushal, S.V. Shah, G.P. Kaushal, Autophagy is associated with apoptosis in cisplatin injury to renal tubular epithelial cells, Am. J. Physiol. Ren. Physiol. 294 (4) (2008) F777–F787.
[15] R. Baliga, Z. Zhang, M. Baliga, N. Ueda, S.V. Shah, In vitro and in vivo evidence suggesting a role for iron in cisplatin-induced nephrotoxicity, Kidney Int. 53 (2) (1998) 394–401.
[16] C.A. Davis, H.S. Nick, A. Agarwal, Manganese superoxide dismutase attenuates Cisplatin-induced renal injury: importance of superoxide, J. Am. Soc. Nephrol. 12 (12) (2001) 2683–2690.
[17] Y. Kawai, T. Nakao, N. Kunimura, Y. Kohda, M. Gemba, Relationship of intracellular calcium and oxygen radicals to Cisplatin-related renal cell injury, J. Pharmacol. Sci. 100 (1) (2006) 65–72.
[18] T. Itoh, et al., Cisplatin induces production of reactive oxygen species via NADPH oxidase activation in human prostate cancer cells, Free Radic. Res. 45 (9) (2011) 1033–1039.
[19] R. Marullo, et al., Cisplatin induces a mitochondrial-ROS response that contributes to cytotoxicity depending on mitochondrial redox status and bioenergetic functions, PLoS One 8 (11) (2013) e81162.
[20] H. Liu, R. Baliga, Cytochrome P450 2E1 null mice provide novel protection against cisplatin-induced nephrotoxicity and apoptosis, Kidney Int. 63 (5) (2003) 1687–1696.
[21] D. Appenroth, S. Frob, L. Kersten, F.K. Splinter, K. Winnefeld, Protective effects of vitamin E and C on cisplatin nephrotoxicity in developing rats, Arch. Toxicol. 71 (11) (1997) 677–683.
[22] G. Sener, et al., The protective effect of melatonin on cisplatin nephrotoxicity, Fundam. Clin. Pharmacol. 14 (6) (2000) 553–560.
[23] D. Ma, et al., Peroxiredoxin I plays a protective role against cisplatin cytotoxicity through mitogen activated kinase signals, Oral Oncol. 45 (12) (2009) 1037–1043.
[24] S.H. Bae, et al., Concerted action of sulfiredoxin and peroxiredoxin I protects against alcohol-induced oxidative injury in mouse liver, Hepatology 53 (3) (2011) 945–953.
[25] T.S. Chang, et al., Peroxiredoxin III, a mitochondrion-specific peroxidase, regulates apoptotic signaling by mitochondria, J. Biol. Chem. 279 (40) (2004) 41975–41984.
[26] H.A. Woo, et al., Reversing the inactivation of peroxiredoxins caused by cysteine sulfinic acid formation, Science 300 (5619) (2003) 653–656.
[27] J. Park, N.H. Kim, H.J. Yi, S.G. Rhee, H.A. Woo, Mitochondrial peroxiredoxin III protects against non-alcoholic fatty liver disease caused by a methionine-choline deficient diet, Antioxidants 12 (1) (2022).
[28] M.O. Iqbal, et al., The nephroprotective effects of Daucus carota and Eclipta prostrata against cisplatin-induced nephrotoxicity in rats, Bioengineered 12 (2) (2021) 12702–12721.
[29] S.J. Holditch, C.N. Brown, A.M. Lombardi, K.N. Nguyen, C.L. Edelstein, Recent advances in models, mechanisms, biomarkers, and interventions in cisplatin-induced acute kidney injury, Int. J. Mol. Sci. 20 (12) (2019).
[30] E. Kwiatkowska, et al., The mechanism of drug nephrotoxicity and the methods for preventing kidney damage, Int. J. Mol. Sci. 22 (11) (2021).
[31] M. Peyrou, P.E. Hanna, A.E. Cribb, Cisplatin, gentamicin, and p-aminophenol induce markers of endoplasmic reticulum stress in the rat kidneys, Toxicol. Sci. 99 (1) (2007) 346–353.
[32] W.X. Ding, et al., Linking of autophagy to ubiquitin-proteasome system is important for the regulation of endoplasmic reticulum stress and cell viability, Am. J. Pathol. 171 (2) (2007) 513–524.
[33] S.A. Tooze, T. Yoshimori, The origin of the autophagosomal membrane, Nat. Cell Biol. 12 (9) (2010) 831–835.
[34] Y. Lu, A.I. Cederbaum, Cisplatin-induced hepatotoxicity is enhanced by elevated expression of cytochrome P450 2E1, Toxicol. Sci. 89 (2) (2006) 515–523.
[35] R. Martinez-Pinna, et al., From tissue iron retention to low systemic haemoglobin levels, new pathophysiological biomarkers of human abdominal aortic aneurysm, Thromb. Haemostasis 112 (1) (2014).
[36] T. Shichita, et al., Peroxiredoxin family proteins are key initiators of post-ischemic inflammation in the brain, Nat. Med. 18 (6) (2012) 911–917.
[37] C.A. Oliveira, et al., An integrated view of cisplatin-induced nephrotoxicity, hepatotoxicity, and cardiotoxicity: characteristics, common molecular mechanisms, and current clinical management, Clin. Exp. Nephrol. 28 (8) (2024) 711–727.
[38] H. Burger, K. Nooter, A.W. Boersma, C.J. Kortland, G. Stoter, Lack of correlation between cisplatin-induced apoptosis, p53 status and expression of Bcl-2 family proteins in testicular germ cell tumour cell lines, Int. J. Cancer 73 (4) (1997) 592–599.
[39] Y.J. Kim, et al., Human prx1 gene is a target of Nrf2 and is up-regulated by hypoxia/reoxygenation: implication to tumor biology, Cancer Res. 67 (2) (2007) 546–554.
[40] Q. Wei, G. Dong, J. Franklin, Z. Dong, The pathological role of Bax in cisplatin nephrotoxicity, Kidney Int. 72 (1) (2007) 53–62.
[41] M. Jiang, C.Y. Wang, S. Huang, T. Yang, Z. Dong, Cisplatin-induced apoptosis in p53-deficient renal cells via the intrinsic mitochondrial pathway, Am. J. Physiol. Ren. Physiol. 296 (5) (2009) F983–F993.
[42] X. Lin, S.B. Howell, DNA mismatch repair and p53 function are major determinants of the rate of development of cisplatin resistance, Mol. Cancer Therapeut. 5 (5) (2006) 1239–1247.
[43] Y.M. Choi, et al., Mechanism of cisplatin-induced cytotoxicity is correlated to impaired metabolism due to mitochondrial ROS generation, PLoS One 10 (8) (2015) e0135083.
[44] R. Fu, et al., Moving beyond cisplatin resistance: mechanisms, challenges, and prospects for overcoming recurrence in clinical cancer therapy, Med. Oncol. 41 (1) (2023) 9.
[45] F.J. Gonzalez, Role of cytochromes P450 in chemical toxicity and oxidative stress: studies with CYP2E1, Mutat. Res. 569 (1–2) (2005) 101–110.